Journal of Pharmaceutical Research International

33(31B): 176-193, 2021; Article no.JPRI.69419
ISSN: 2456-9119
(Past name: British Journal of Pharmaceutical Research, Past ISSN: 2231-2919, NLM ID: 101631759)

Surface Modification of Optimized Asenapine Maleate Loaded Solid Lipid Nanoparticles Using Box-Behnken Design

A. Rekha Devi[1], M. Vidyavathi[1*] and S. P. Suryateja[2]

[1]Department of Pharmaceutics, Institute of Pharmaceutical Technology, Sri Padmavati Mahila Viswavidyalayam, Tirupati, 517502, India.
[2]Indegene Pvt. Ltd., Bangalore, India.

Authors' contributions

All the authors are collaboratly performed this research work. Corresponding author drafted the manuscript. All authors read and approved the final manuscript.

Article Information

DOI: 10.9734/JPRI/2021/v33i31B31706
Editor(s):
(1) Dr. Vasudevan Mani, Qassim University, Kingdom of Saudi Arabia.
Reviewers:
(1) Mahdi Jufri, Faculty of Pharmacy Universitas, Indonesia.
(2) Mothilal M, SRM College of Pharmacy, SRM Institute of Science and Technology, India.
Complete Peer review History: http://www.sdiarticle4.com/review-history/69419

Original Research Article

Received 01 April 2021
Accepted 09 June 2021
Published 15 June 2021

ABSTRACT

Aim: The aim of the present study was to design and evaluate solid lipid nanoparticles of Asenapine maleate (<2% bioavailability) to enhance its oral bioavailability and surface modification for brain targeting.
Methods: A modified solvent injection method was used to produce Asenapine maleate loaded solid lipid nanoparticles. A RSM 3-factor, 3-level Box-Behnken design was applied to study the effect of three independent variables, concentrations of lipid (A), drug (B) and surfactant (C) on three dependent variables, particles size (Y1), entrapment efficiency (Y2), and drug release (Y3). 3-D surface response plots were drawn and optimized formulation was selected based on desirability factor. Then it was coated with tween 80 for ease of permeability through blood brain barrier due to intact absorption of solid lipid nanoparticles.
Results: The results of coated optimized formulation showed average particle size of 108.9 nm, entrapment efficiency of 78.62%, and *in vitro* drug release of 98.88±0.102% at 36 hr at pH 7.4. Morphologically, particles were almost spherical in shape with uniform size distribution. Targeting of coated optimized formulation to brain after oral administration was confirmed by fluorescence

**Corresponding author: E-mail: vidyasur@rediffmail.com;*

microscopy studies on male albino wistar strain rats. This research also envisaged that there is a >85% cell viability up to 125µg/ ml concentration of coated solid lipid nanoparticles by MTT assay.
Conclusion: Thus, the current study successfully designed, developed an optimized SLN formulation of Asenapine maleate using a 3-factor, 3-level Box-Behnken design for brain targeting to treat Schizophrenia by bypassing the first pass metabolism with enhanced oral bioavailability.

Keywords: SLNs; asenapine maleate; schizophrenia; fluorescent microscopy; enhanced bioavailability; brain targeting; box-behnken design.

1. INTRODUCTION

Nanocarrier based drug delivery has gained more attention as a reliable technique to significantly improve the bioavailability (BA) of lipophilic drugs. In addition, nanocarriers also provide a platform to change drug internalization pathway and protects gastric degradation. In particular, lipid-based nanocarriers approach proven to be highly efficient in improving BA of poorly water-soluble drugs by alternate absorption pathway along with exceptional drug release properties [1]. Solid lipid nanoparticles (SLNs), comprising drug entrapped with biocompatible lipid, serves as a potentially successful alternate to overcome the pitfalls of oral drug delivery [2]. Due to its colloidal nature and particle size SLNs, offers plethora of desired biopharmaceutical advantages, like drug targeting and improved therapeutic efficiency [3].

Asenapine maleate (AM), a second generation (atypical) antipsychotic agent, is generally used in treating schizophrenia patients due to the strong inhibitory action on $5HT_2A$ (serotonin) and D_2 (dopamine) receptors. Despite its strong affinity towards the receptors, its pharmacological action is often comprised by poor aqueous solubility and metabolic pathway. In clinical scenario, AM exhibited oral BA of less than 2% and can be highly attributed to its BCS class II nature and CYP1A2 metabolic pathway [4]. However, as an alternate dosage form, AM is available as sublingual tablets with BA of 35% [5]. But a major setback was observed in the clinical practice due to poor patient compliance an account of its organoleptic properties [6]. Considering these circumstances, an alternate dosage form is essential to overcome the earlier drawbacks. We hypothesise that AM as orally administrable SLNs can improve the BA by avoiding the first pass metabolism and can also nullify the undesirable organoleptic properties. Further, presently following lipid-based approach is instrumental in improvement of brain specific delivery of AM due to intact absorption.

In addition to the hurdles in robust preparation of nanocarriers, the BA of the drug loaded SLN also depends on its particle size, charge and drug release. Studies have previously reported that Design of Experiment (DoE) based approach gives exceptional control over the nanoparticle properties. The current research work focuses on the fabrication of AM loaded SLNs by employing the DoE technique for improving the BA. The novelty of study was the surface modification of nanoparticles with tween 80 to enhance the penetration of SLNs into the brain. The study investigated the brain targeting ability of coated AM-SLNs by bio distribution studies [7]. This research also envisaged the cell viability of coated solid lipid nanoparticles by MTT assay.

2. MATERIAL AND METHODOLOGY

2.1 Materials

Asenapine Maleate is a gift sample from Lee Pharma Limited, Hyderabad. Tristearin (90%-Assay) and Lecithin soya (30%) were purchased from Himedia Laboratories Pvt. Ltd., Mumbai. Double distilled water is used throughout the study. MTT Kit (Sigma Aldrich). All other chemicals and materials utilized were analytical reagent (AR) grade.

2.2 Methodology

2.2.1 Experimental design

The box behnken method was employed in the current study and was framed with 12 factorial points and 5 replicates to achieve fraction of design space (FDS) more than 80%. The FDS was calculated based on the primary developmental goal of constructing design space for robust preparation of smaller nanocarriers [8]. From the preliminary screening test, it was found that the drug concentration (*A*), lipid concentration (*B*), Surfactant concentration(*C*) [9], had a significant effect on the particle size

(*Y1*), % entrapment efficiency (*Y2*) and % Drug Release (*Y3*) of SLNs [10]. Therefore, by fixing the stirring speed (2000rpm), stirring time (1h) and sonication time (1min), the effect of three selected variables (*A*), (*B*), and (*C*) was studied at three different levels, low (-1), medium(0), and high(-1) in (Table 1) [11].The coded and actual values of the variables are given in (Table 2). The following second-order polynomial equation was used to draw conclusion after considering the magnitude of coefficient and mathematical sign as follows:

$$Y= \beta_0+ \beta_1A+ \beta_2B + \beta_3C + \beta_{11}A^2 + \beta_{22}B^2 + \beta_{33}C^2 + \beta_{12}AB+ \beta_{13}AC + \beta_{23}BC$$

Where *Y* was predicted response(s), β_0 was an intercept, β_1, β_2, and β_3 were linear coefficients, β_{11}, β_{22}, and β_{33} were squared coefficients and quadratic term, β_{12}, β_{13}, and β_{23} were interaction coefficients, and *A, B,* and *C* were independent variables, which were selected based on the results from a preliminary study. Predicted $R^2$and adjusted R^2 were evaluated to find the fitness of the model [12].

2.2.2 Optimization of SLNs by DoE:

Considering the study objective of establishing design space, the tolerance intervals were considered for optimization of particle size with maximum drug entrapment. Preferring tolerance intervals will be beneficial in prediction with lesser variations. Among software predicted numerical solution obtained after optimization, the more experimental feasible solution was chosen for validation. Solutions near the extremities of design space were not considered for validation in order to build a reliable design space. The predicted combination which lies in the sweet spot, (simultaneous meeting point of desired response) with maximum desirability was conducted. The experiment was conducted in triplicate and the experimentally obtained responses were compared with the predicted responses to validate the model.

2.2.3 Preparation of AM SLNs

In a preliminary study, various factors like lipid concentration (50-70 mg), drug concentration (5-10 mg), surfactant concentration (Tween 80, 0.1-0.3mL), stirring time (1 h), stirring speed (2000rpm), and sonication time (1 min) were fixed and their effect on particle size (nm), entrapment efficiency (%) and drug release (%) was determined by the software; Design-Expert, 10v.as shown in (Table 1) and a total of 17 formulations were prepared as per design (Table 2). AM SLNs were prepared by a slight modification of the previously reported modified solvent injection method. Lipids (tristearin and soya lecithin) were dissolved in ethanol with continuous stirring at 60ºC and AM drug was added to organic phase. An aqueous phase was prepared by dissolving surfactant in phosphate buffer solution (PBS) pH 7.4 and maintained at same temperature of organic phase (60ºC). Hot organic phase was added to aqueous phase with the aid of 24G needle syringe under continuous stirring (Remi Instruments, India) at constant speed (2000rpm) for a duration of 1 h and maintained at 60ºC as depicted in Fig.1. This led to the formation of a dispersion, which was then filtered with a whatman filter paper in order to remove excess lipid and ultra-sonicated using a probe sonicator (Lark innovative technology, Chennai) and cooled to room temperature for SLNs formation [13].

Table 1. Variables and their levels in Box-Behnken design

Variables	**Levels of variables**		
Independent variables	**Low (-1)**	**Medium (0)**	**High (+1)**
(A)Lipid concentration (mg)	50	60	70
(B)Drug concentration (mg)	5	7.5	10
(C) Surfactant concentration (mL)	0.1	0.2	0.3
Dependent variables	**Goals**		
(Y1) Particle Size (nm) – PS(nm)	Minimize		
(Y2) Entrapment Efficiency (%) – EE%	Maximize		
(Y3) Drug Release (%) - DR%	Maximize		

Table 2. Observed responses for 17 runs of AM SLNs according to Box-Behnken design

Formulation Code	Lipid (Tristearin) (mg)	Drug (AM) (mg)	Surfactant (Tween-80) (mL)	PS(nm)	EE(%)	DR(%)
F1	+1	0	+1	160.5±2.33	63.5±1.32	89.5±1.35
F2	0	0	0	108.5±2.89	74.3±0.56	97.2±1.09
F3	0	-1	-1	110.3±2.97	73.5±1.03	96.2±1.84
F4	+1	+1	0	153.4±2.56	64.3±1.98	91.2±1.43
F5	+1	-1	0	148.2±2.67	69.1±0.45	88.4±0.47
F6	0	0	0	102.4±2.36	73.1±0.78	96.7±0.69
F7	0	-1	+1	121.3±2.59	72.5±0.89	95.8±1.45
F8	+1	0	-1	142.7±2.32	63.9±1.32	92.7±1.64
F9	-1	0	-1	126.9±2.54	68.9±1.74	94.5±1.84
F10	-1	+1	0	106.7±2.87	71.6±1.82	95.4±1.53
F11	0	+1	-1	124.6±2.65	62.5±0.98	97.6±1.65
F12	0	0	+1	105.8±2.61	73.9±1.37	96.8±1.47
F13	0	+1	+1	110.4±2.87	69.2±1.63	97.8±0.89
F14	0	0	0	112.7±3.16	72.9±1.48	96.4±1.81
F15	0	0	0	104.2±1.12	71.3±1.73	97.4±1.30
F16	0	0	0	103.6±3.23	72.8±1.06	97.5±1.37
F17	-1	-1	0	120.8±1.33	77.9±0.69	96.2±0.83

(n=3, mean ± SD)

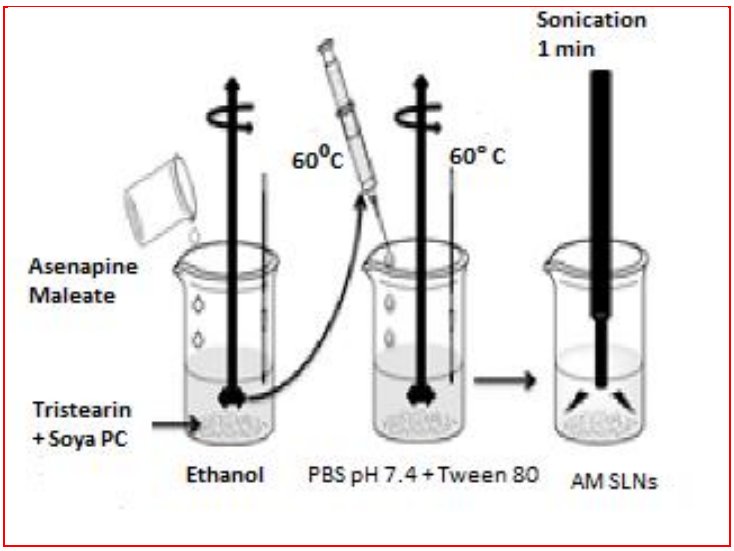

Fig. 1. Preparation of AM SLNs

2.3 Physical Characterization Methods

2.3.1 Particle size, polydispersity index, and zeta potential

All samples were diluted in 1:10 ratio with deionized water to get optimum counts. Average particle size (PS), PDI and zeta potential (ZP) were measured by Zetasizer, (HAS 3000; Malvern Instruments, Malvern, UK). Measurements were carried out with an angle of 90º at 25ºC [14].

2.3.2 Entrapment efficiency

It was determined by size exclusion method (Sephadex G – 50 mini column). 2 ml of SLN dispersion was applied drop wise on the top of the column and then centrifuged at 2000rpm for 2 minutes at room temperature (Remi Instruments Pvt. Ltd, India), to expel and remove void volume containing SLN into the centrifuged tubes. This eluted dispersion was lysed by disrupting with 0.1% Triton X-100 and the amount of entrapped drug was analysed spectrophotometrically at λmax 269nm (Shimadzu 1800, Japan) and was calculated [15].

$$\%EE = \frac{\text{Total drug} - \text{Unentrapped drug}}{\text{Total drug}} X100$$

2.3.3 In-vitro drug release studies

Overnight soaked dialysis membrane (Hi-media, molecular weight cut-off 12,000 Daltons) was tied to one of the opening of two side opened boiling tube. 1 ml of SLN suspension free from unentrapped drug was placed in dialysis tube, which was suspended in a 200ml of PBS, pH 7.4 and placed on magnetic stirrer at the temperature of 37 ± 2 ° C with continuous stirring at moderate speed (dialysis membrane/ diffusion method). At specified time intervals i.e 0.5hr, 1 hr, 2 hr, 4hr, 6hr, 12hr and 24hr, the 5 ml of samples were collected and analysed by spectrophotometrically at λmax 269nm [16].

2.4 Coating of Optimized Formulation

Surface modification of optimized SLNs (OF3) was processed using 1% (w/v) polysorbate 80 (Tween® 80) solution. It was admixed to nanoparticles suspension for surface coating under magnetic stirring for 30 min. Resultant coated nanoparticles were centrifuged, redispersed and was stored under refrigerated condition for further characterization [17].

2.4.1 Physical characterization of coated optimized formulation (COF)

Along with the physical characterization studies of PS, PDI, ZP, EE and DR, the following studies were also performed on COF.

2.4.1.1 Field Emission-scanning electron microscopy (FE-SEM)

The surface morphology of COF was studied using FE-SEM (BRUKER, x-Flash 6130, USA) at 25 ± 2°C. The SLN dispersion was placed on

silicon wafer and dried for 24 h. Further, it was analysed at 50.000 magnifications with accelerating voltage of 10 kV [18].

2.4.1.2 Fourier-transform infrared spectroscopy (FTIR) studies

FTIR studies of AM (pure drug) and COF were carried out to evaluate any changes in the principal functional groups of drug and for confirmation of entrapment of drug in lipid. The study was conducted on IR spectrophotometer (Shimadzu, FTIR 8700), in the frequency region of 400 to 4000 cm-1 by the direct sampling method [19].

2.4.1.3 Liquid X-Ray diffraction (XRD) studies

XRD studies of AM (pure drug) and COF were carried out to check the crystallinity of drug in pure and SLNs. The study was performed on a Siemens DIFFRAC plus 5000 liquid diffractometer with CuKα radiation (1.54056 A). The tube voltage and amperage were set at 40 kV and 40 mA, respectively. Each sample was θ-2θ scanned between 10° - 40° with a step size of 0.01° at 1 step [20].

2.4.1.4 Differential scanning calorimetry (DSC) studies

DSC studies of AM (pure drug) and COF were carried out to evaluate any change in drug with respect to melting enthalpy, glass transition temperature and any interactions with excipients. The study was carried on DSC Q1000, TA instrument. About 2-5 mg of sample was placed in standard aluminium pans and scanned in the range from 5 °C to above its melting point with temperature increment speed of 10 °C/min under the dry nitrogen used as effluent gas (flow rate 50 ml/min) [21].

2.5 Biodistribution Studies by Fluorescence Microscope

SLNs were prepared using fluorescence dye (10ng/mL) to entrap fluorescence marker into SLN in place of AM by modified solvent injection method as discussed previously. The fluorescence microscopy was performed with intent to confirm the delivery of the AM loaded SLNs to liver, kidney and brain. Male albino rats (Wistar-derived strain) weighing 150–200 gm were chosen for the present studies. The rats were divided into two groups each containing three animals. First group was treated with plain dye solution administered via oral route. The dye entrapped optimized SLNs dispersion was administered the animals of second group orally. Rats were sacrificed at 0.5hr, 12hr and 36hr and brain was excised and isolated. It was cut into small pieces and washed with Ringer's solution followed by subsequent drying using tissue paper. Dried pieces of liver, kidney and brain were then fixed in Carnay's fluid (absolute alcohol: chloroform: glacial acetic acid; 3.5:1:0.5). Prepared blocks were cut into the sections using microtome and analysed under fluorescence microscope [22]. All studies on animals were approved by IAEC, Sri Padmavathi School of Pharmacy, Tiruchanoor. (IAEC No:SPSP:1016/PO/Re/S/06/CPCSEA/2017/ 014).

2.6 Cytotoxicity Test using Caco-2 cells

MTT assay was conducted to determine the cell viability at different concentrations of COF.

0.5 mg/ml of MTT (Sigma, M-5655) was prepared in PBS and sterilized by filtration sterilization. Incubated $1.5x10^4$ Caco-2 cells / well on 96 well tissue culture plate with the various concentrations of test (COF) and control (AM suspension) for 24hrs. After the incubation period, the supernatant of each test and control wells, was removed and mixed with 100µl of MTT and solution, the plate was gently shaken well and then incubated at 37ºC in a humidified 5% CO_2 incubator for 4 hours. The wells were mixed gently with DMSO by shaking up and down in order to solubilize the formazan crystals formed by MTT. Then, the absorbance was measured by using micro plate reader at a wavelength of 570 nm [23].

The percentage of growth inhibition was calculated using the formula:

$$\%\ \text{of cell viability} = \frac{\text{Mean OD of Test}}{\text{Mean OD of Control}}\ X\ 100$$

3. RESULTS AND DISCUSSION

3.1 Assessment of Prediction Capability

FDS is the measure of the percentage ability of the design space to predict with minimum variance. Based on the standard deviation observed from previous investigations, the FDS was found to be 98% at $P<0.05$ and was greater than the general recommendation (FDS>80%). Higher FDS evidenced that the reliable exploration and optimization results can be obtained from the study (Fig. 2) [24].

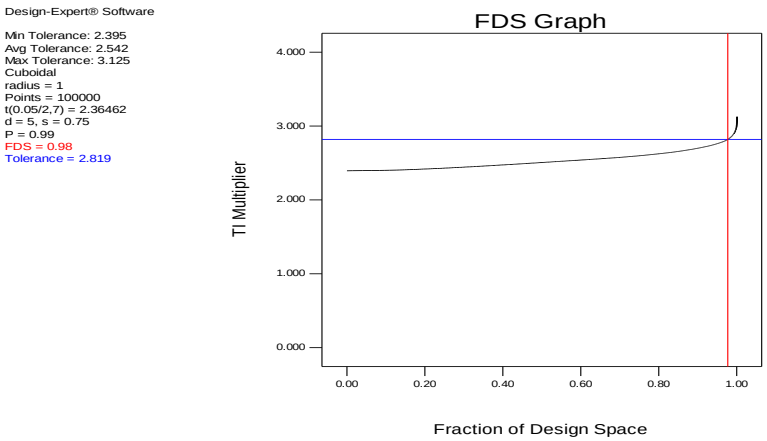

Fig. 2. Design space measurement

3.1.1 Particle size

The fabricated AM-SLNs were ranging from 103nm to 168nm depending on the amount of formulations variables included in the formulation. The SLNs were lipophilic in nature. Quadratic model was selected for the model construction, and the respective *P*-value was found to be <0.01. The descriptive statistics like R^2, adjusted R^2, predicted R^2 elucidate the ability of model for optimization were shown in (Table 3). The significant *P*-value of the lipid endorsed that particle size was significantly influenced by the lipid concentration. Surprisingly, perturbation chart (Fig. 3) revealed that the lipid concentration was found to have valley type curvature effect on particle size. As the amount of lipid rises, the particle size tend to decrease, but after certain concentration, the particle size increased enormously. Curvature effect observed can be attributed to the drug enriched core type formation of SLN leading to reduced particle size. However, enlargement of particle size beyond optimum concentrations of lipid could be due to lipid accumulation [25]. Furthermore, the interaction of lipid with surfactant was non-significant but indispensable which was evident from the contour plots. Predicted Vs Actual graph indicated the smaller variance and efficient approximation from the fitted quadratic model. Moreover, the decreasing particle size at high surfactant could be owed to the decreased coalescence between the particles.

3.1.2 Entrapment efficiency

Achieving high drug entrapment efficiency is pivotal in determining the dose and efficiency of the formulation. All the formulations exhibited excellent drug entrapment in the SLNs. All the formulations exhibited good EE with a minimum of being 61% and were a suggestive of effective drug loading. Similar to particle size, the quadratic model was fitted for constructing the prediction equation and the descriptive statistics were mentioned in the table. Excellent descriptive statistics of the model indicated precision, goodness of fit and interpolation ability of the model. Despite high drug concentrations, only limited amount of API was entrapped in the SLN due to formation of drug enriched core with drug loss and attributed to negative effect between them. Meanwhile, an increase in %EE from 63.5% (F1) to 74.3% (F2) with decrease in surfactant ratio was due to the similar effect. Furthermore, perturbation chart (Fig. 4) exposed that beyond certain level, high concentrations of lipid competed with the API during the SLN formation.

3.1.3 *In vitro* drug Release studies

Under sink conditions, AM-SLNs exhibited typical biphasic release pattern with an initial burst release followed by slow and prolonged release. The initial burst release could be due to the drug adsorbed on the lipid surface during preparation. The prolonged drug release observed elucidated the formation drug enriched core model which could be attributed more towards the differences in melting point between the lipid and drug. The lipid soluble drug has higher melting eventually crystallizing first, leaving the lipid to crystallize to form as a wrapping layer. Furthermore, higher concentration of lipid in the formulation also could have attributed to the model and facilitating retarded drug release for longer time periods.

Table 3. ANOVA results for AM loaded SLNs

Source	PS		EE	DR
Model	0.001	Significant	0.004	0.005
A-Lipid	< 0.001		< 0.001	< 0.001
B-SURF	0.003		0.011	0.016
C-Drug	0.081		0.481	0.798
AB	0.453		0.028	0.890
AC	0.008		0.059	0.263
BC	0.081		0.259	0.140
F Value	46.64		39.52	46.49
P Value	<0.001		<0.001	<0.001
Lack of Fit	0.38		0.46	0.23
P Value	0.776		0.740	0.252
R^2	0.984		0.981	0.984
Predicted R^2	0.922		0.901	0.831
Adjusted R^2	0.963		0.956	0.962
Adequate Precision	345.973		21.26	20.585

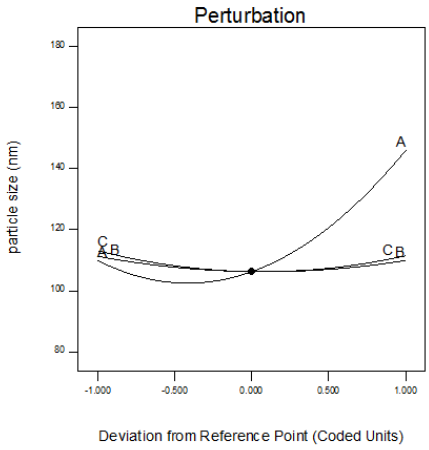

Fig. 3. Effect of A, B and C on Particle size

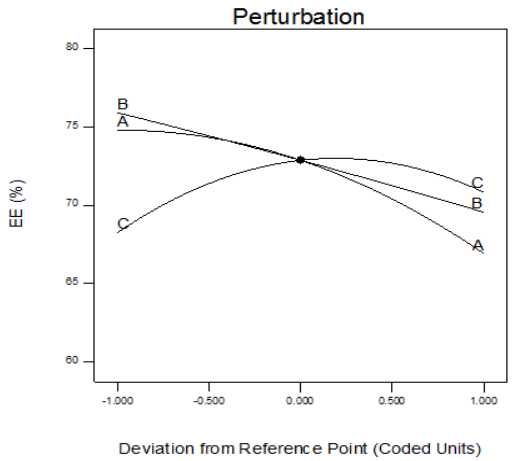

Fig. 4. Graph showing the effect of A, B and C on entrapment efficiency

Drug release pattern also was best explained by the quadratic model and high regression values showcased the excellent predictive ability of the model. Apart from the main effects, interaction effects were also commanding which was evidenced from the contour plots. Due to superior dominance of significant main variable effects on the drug release, interaction effects also had greater impact on the drug release. Similar trends in interaction effects were observed for the particle size and the EE. Apparently, unavoidable inter dependency of lipid and surfactant in determining key elements like extent of API solubility, viscosity during preparation and formation of SLN core could be the reason for interaction effects observed in the model. However, negative impact of higher levels of lipid, surfactant concentrations was observed and could be attributed to the formation of more stable SLN with drug in the inner core [26]. As a generally expected phenomenon, elevated drug release at high drug concentration was observed in the current study and was evident from the formulations F5 and F4.

However, a significant interaction effect among the variables (Fig.5) was also observed from curved lines of contour plots and will be pivotal in optimization criteria.

3.2 Optimization

Nanocarriers were optimized for smaller particle size with enhanced drug loading for enhanced brain targeting. Drug concentration was fixed at 5mg based on the effects observed in experimental runs for higher drug concentrations. Preparation of nanocarriers with small particle size was given more priority and was followed by maximizing the drug release within the explored design space of variables. Among the solutions, the experimental combination with high derringer desirability and experimental feasibility was chosen to validate the model for predictive ability (Table 4 and 5). In addition, as mentioned in the figure, the combinations at the extremities in the design space with tolerable intervals were not considered (Fig. 6-8).

The second order polynomial equation relating the response of particle size (Y1), % entrapment efficiency (Y2) and % drug release (Y3) was given below:

PS =+106.28 + 18.08 * A -0.69 * B - 0.81 * C + 4.82 * AB +9.73 * AC - 6.30 * BC +21.66 * A^2 + 4.33*B^2 +6.04 * C^2.

%EE = +18.495 +2.18175 * A - 3.37* B +168.72 *C +0.015 * AB -1.35*AC+7.70 * B C – 0.0202 * A^2 – 0.022 * B^2– 3.32* C^2.

% DR : -29.83 + 4.37 * A – 1.09 * B + 68.93 * C +0.04 * AB – 1.38 * AC +0.60 * BC – 0.039 * A^2- 0.061 * B^2 +19.25 * C^2.

3.3 Physical Characterization of COF:

Particle size, size distribution & zeta potential curve of COF are shown in Fig. 9 & 10 respectively. The average particle size, PDI and zeta potential were found to be 108.9 nm, which has brain permeability (≤200nm), 1.217 showed an broader particle distribution and -24.3 mV indicates that prepared SLNs were stable respectively due to high surface charge (Fig. 9a, Fig. 9b). The % entrapment efficiency and % drug release at 36 h in pH 7.4 PBS of COF was found to be 74.92% and 96.48% respectively (Table.2), this may be due to the strong layer coated on the SLNs by Tween 80. The particle shape is almost spherical (Fig 9c). The characteristic peaks of drug such as of aromatic C-H stretch (3036 cm^{-1}), C-H stretch of methyl group (2925 cm^{-1}), C=O (1706 cm^{-1}), C-C stretch (1618, 1484 cm^{-1}), C-O stretching (1293 cm^{-1}), C=C stretch (1093 cm^{-1}), and aromatic C-Cl bends (655 and 587 cm^{-1}) disappeared and were replaced by the peak of tristearin (lipid). Remaining peaks also either shifted or replaced in the IR spectrum of COF are shown in Fig.10. This established the drug entrapment in a lipid matrix and the compatibility between the drug and excipients used in the formulation.

3.4 Differential Scanning Calorimetry (DSC)

The melting point of AM (pure drug) was significantly decreased 147.50°C to 55.03°C in COF, due to drug entrapment in the lipid and lead to lowering of melting point may be addition of excipients. As lipid enclosed the drug, first the melting point of lipid was showed a peak at 55.03°C (Fig. 11). Studies manifested that the majority of the SLNs are less ordered arrangement of crystals lead to amorphous nature in dissolved status within lipid which confirmed the loading of drug.

3.5 Liquid X-Ray Diffraction Study

Lecithin can transform the properties of matrix SLNs. Hence the melting and crystallization depends only by hard lipid component. The pure drug presented sharp peaks at 2Θ of 8.7, 20.6,

21.3, 25.0 and 28.3 augurs that the pure drug AM is crystalline. The AM loaded SLNs crooked peak exhibiting SLNs are in amorphous nature. (Fig.12) [27].

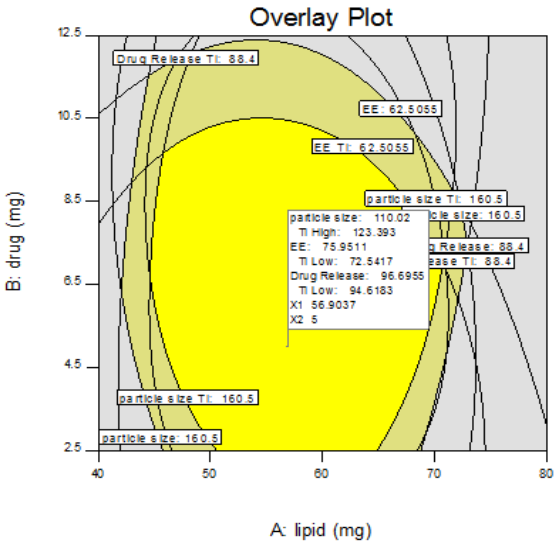

Fig. 5. The overall plot of A, B, and C effect on Y1, Y2 and Y3.

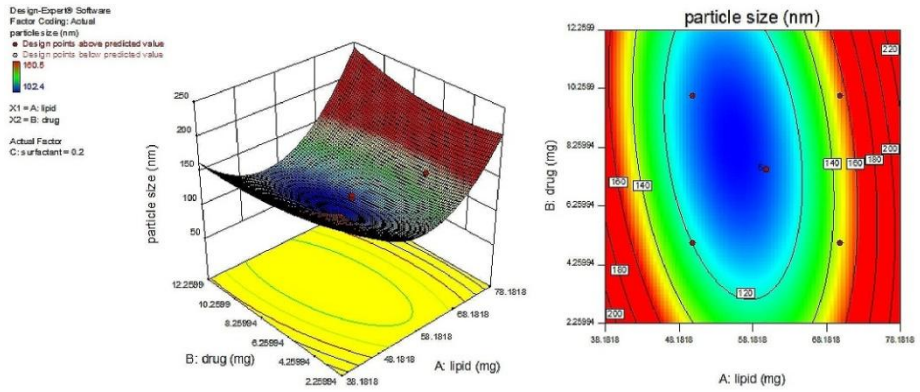

Fig. 6. 3-D surface response and contour plot of particle size (nm)

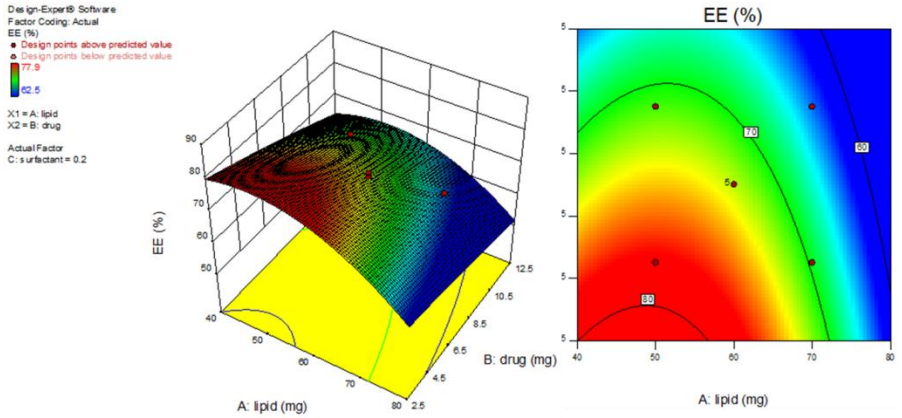

Fig. 7. 3-D surface response and contour plot of entrapment efficiency (%)

Table 4. Regression analysis for particles size, entrapment efficiency and drug release

Factor	Particle Size (nm)		Entrapment Efficiency (%)		Drug Release (%)	
	Coefficient (β)	*P*-value	Coefficient (β)	*P*-value	Coefficient (β)	P-value
Intercept	106.28		72.88		97.04	
A	18.07	< 0.001	-3.94	< 0.001	-2.64	< 0.001
B	-0.69	0.611	-3.16	< 0.001	0.68	0.012
C	-0.81	0.549	1.29	0.006	-0.14	0.515
AB	4.83	0.033	0.38	0.447	0.90	0.016
AC	9.73	0.001	-1.35	0.023	-1.38	0.002
BC	-6.30	0.011	1.93	0.004	0.15	0.613
A^2	21.66	< 0.001	-2.02	0.003	-3.86	< 0.001
B^2	4.34	0.045	-0.14	0.767	-0.38	0.209
C^2	6.04	0.012	-3.32	0.002	0.19	0.508

Table 5. Point prediction check point for optimization, actual value, experimental value and % error

Formulation Code	Composition of optimized formulation (OF)			Response	Actual Value	Predicted value	% Error
	Lipid (Tristearin - mg)	Drug (AM - mg)	Surfactant (Tween 80 - mL)				
OF1	56.07	5	0.1	Y1	110.23± 2.01	111.25	0.92
				Y2	74.96±0.95	75.73	1.02
				Y3	95.92±2.18	96.69	0.80
OF2	55.59	5	0.11	Y1	112.60±3.85	113.89	1.14
				Y2	75.02±1.92	74.53	0.66
				Y3	95.08±0.68	96.66	1.64
OF3	55.84	5	0.11	Y1	111.30±2.04	112.64	1.19
				Y2	74.92±1.15	75.13	0.28
				Y3	96.48±0.93	96.66	0.18
OF4	55.93	5	0.1	Y1	108.90±5.12	111.00	1.89
				Y2	72.98±6.73	75.64	3.51
				Y3	94.65±3.61	96.68	2.10
COF	55.84	5	0.11	Y1	108.9±0.28	-	-
				Y2	78.62±0.51	-	-
				Y3	98.88±0.102	-	-

(n = 3, mean ± SD)

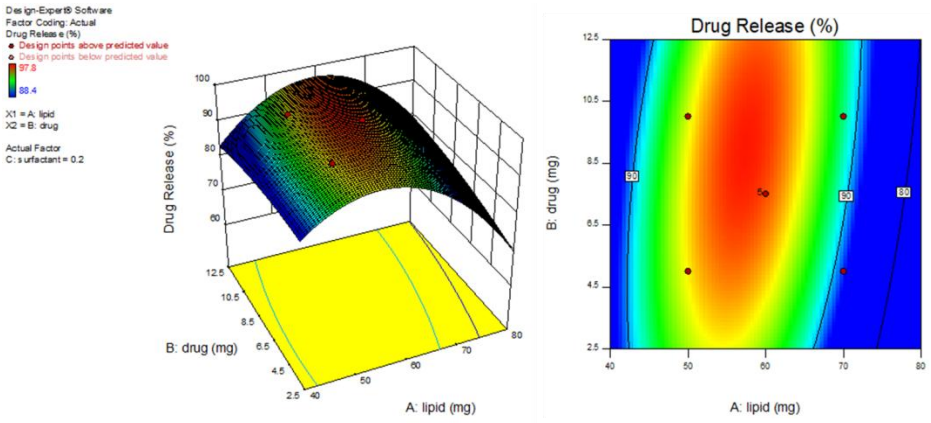

Fig. 8. 3-D surface response and contour plots of drug release (%)

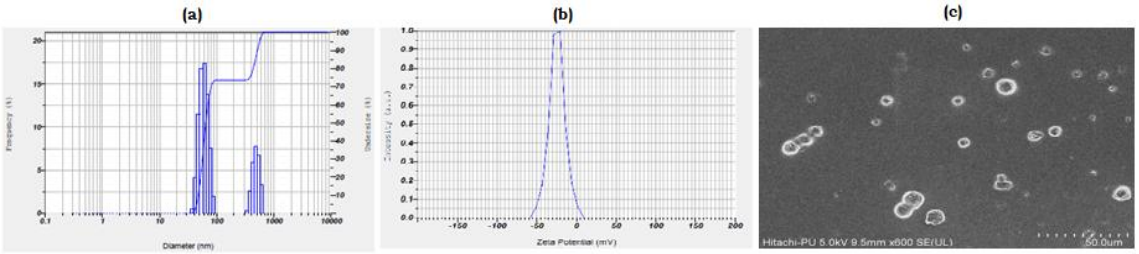

Fig. 9. (a) Particle size distribution curve, (b) Zeta potential curve and (c) FE-SEM images of coated optimized AM SLNs

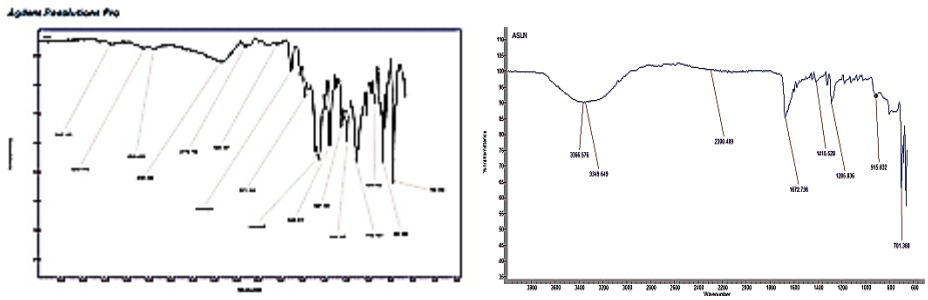

Fig. 10. FTIR of AM (pure drug) and ASLN (coated optimized SLNs)

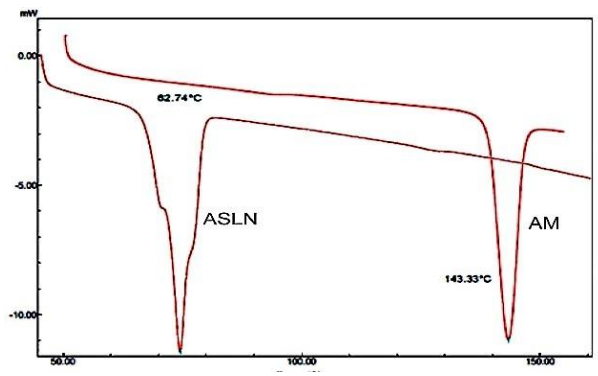

Fig. 11. DSC images of AM (pure drug) and ASLN (coated optimized SLNs)

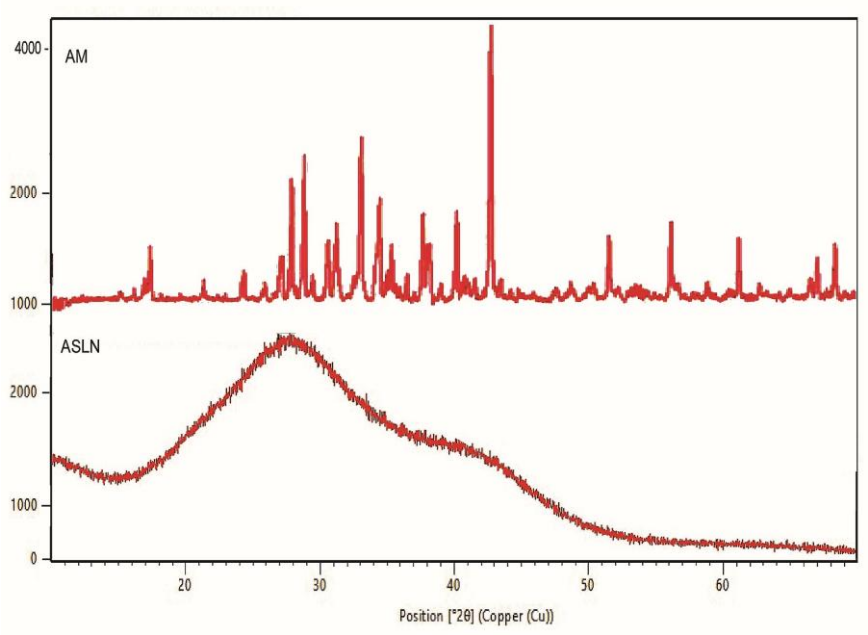

Fig. 12. XRD pattern of pure drug (AM) and coated optimised SLNs (ASLN)

3.6 In-vitro Drug Release Kinetics

The drug release of the OF3 was observed up to 24hrs, whereas the drug release from COF was 36hrs indicating that due to surface modification, the drug release is sustained (Fig.13). The release kinetics of OF3, COF was applied for various kinetic models by using PCP Disso V3.01 software. The best fit model for both is Korsmeyer-Peppas. n=0.5282 (OF3), 0.449(COF), and k=16.0802, 15.3936 for OF3 and COF respectively. Where n = 0.5, is an indicative of release mechanism (slow diffusion) of AM from SLN matrix, which depicts that this fits in time dependent Fickian diffusion drug release from insoluble lipid matrix. The best linearity was followed by the matrix kinetics (R^2 – 0.9809, 0.9873) as shown in Table 6 [28].

3.7 Field Emission Scanning Electron Microscopy (FESEM):

Measurement of the solid lipid nanoparticles for surface topography was clearly explains the internal structure with the FE-SEM. Image (Fig. 14) showed that the SLNs formed are almost spherical in nature [29].

3.8 Biodistribution Studies by Fluorescence Microscope

The results depicted an increased deposition of fluorescent dye loaded SLN in liver and kidney of the rodents. However, with increase in time, the accumulation of SLN in brain tissue was increased which could be an indication of the improved ability to cross BBB. As host defence mechanism recognise the systemic SLN with bigger particle size as antigens and could be the reason for spike in SLN deposition in the liver and kidneys in the first few hours shown in Fig.15 [30]. Physiologically, these organs act on the foreign substances and help in neutralizing them. However, the smaller particle size of SLNs would have been instrumental in bypassing the host defence mechanism and cross BBB due to their lipid core, eventually delivering the drug payload in the brain tissue [31].

3.9 Cytotoxicity Test using Caco-2 cells

MTT assay results prudent that prepared SLNs were non-toxic as it showed that CaCo-2 cells viability was not significantly decreased as that of pure drug suspension. Cell viability observed as concentration dependent. There was a decrease in cell viability after 125µg/ml (Fig.16) which may be due to surfactant coating. Hence, it proven that there is no cytotoxicity up to 125µg/ml [32].

In this study, all of the experiments were performed in triplicate and the average values were considered as the response.

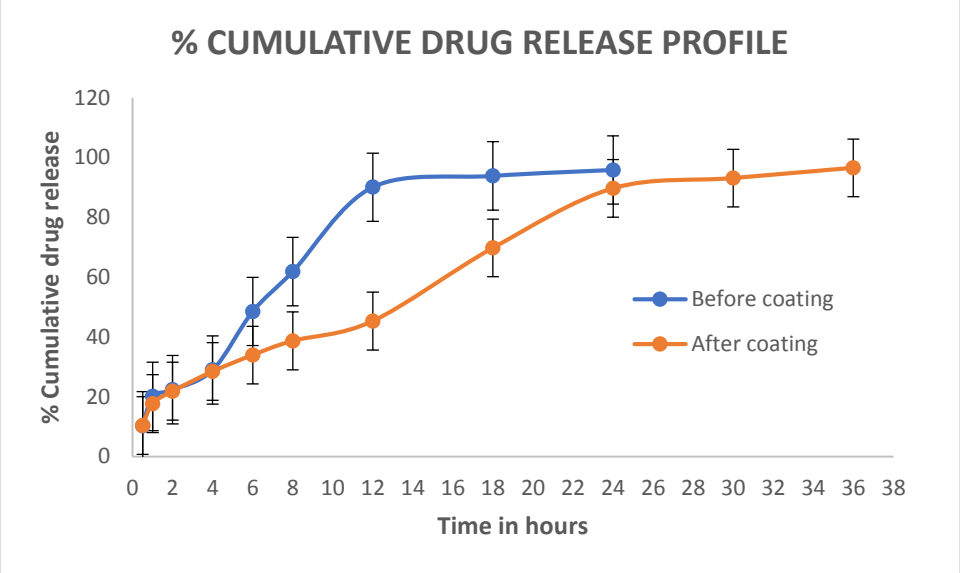

Fig. 13. *In-vitro* drug release of (OF3) before coating, (COF) after coating of SLNs

Table 6. Drug release kinetics values for model fitting

Kinetics model	Model Fitting (Average) Values for OF3		Model Fitting (Average) Values for COF	
	R	K	R	K
Zero order	0.859	4.288	0.897	2.717
T-test	4.750	(Passes)	6.450	(Passes)
1st order	0.962	-0.078	0.983	-0.049
T-test	10.039	(Passes)	17.193	(Passes)
Matrix	0.981	17.500	0.987	13.605
T-test	14.264	(Passes)	19.614	(Passes)
Peppas	0.981	16.080	0.981	15.393
T-test	14.510	(Passes)	16.240	(Passes)
Hix.Crow.	0.940	-0.021	0.971	-0.013
T-test	7.813	(Passes)	12.874	(Passes)

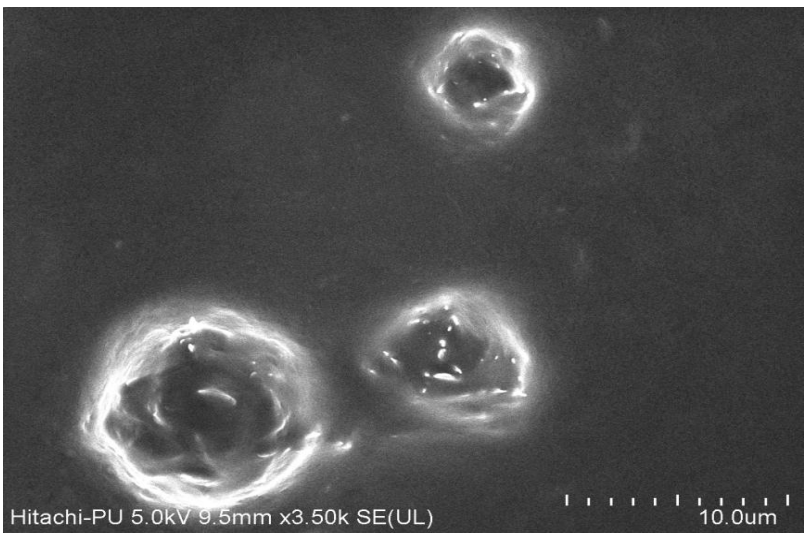

Fig. 14. Surface morphology of COF

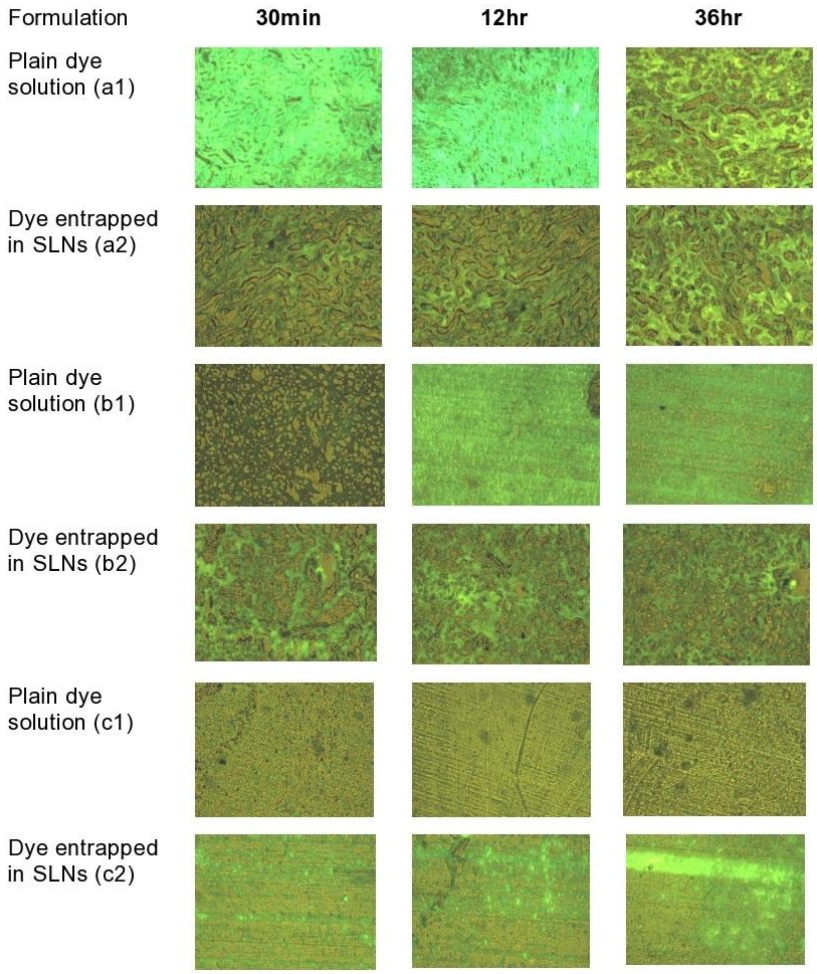

Fig. 15. (a1,a2) Kidney, (b1,b2) Liver and (c1,c2) Brain fluorescence microscopy images at 30 min, 12 h and 36 h after oral administration of plain dye solution and dye entrapped in COF to male albino wistar strain rats

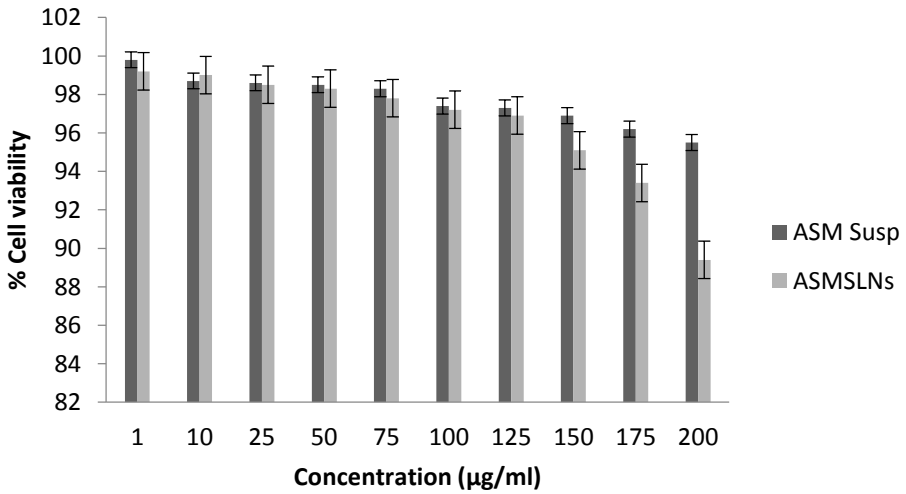

Fig. 16. Results of %cell viability in MTT Assay

4. CONCLUSION

In this study, the SLNs for AM were designed and prepared by the modified solvent injection method. The SLNs were optimized using the 3-level 3-factor Box-Behnken statistical design. The increased drug content may also result in decrease particle size in the drug enriched core. Contour plots reveal that the lipid and the API have interaction with surfactant and is the reason for curvature effect of lipid in determining particle size. The optimized formulation (OF3) was coated with 1% w/v solution of polysorbate 80. The coated optimized formulation (COF) exhibited particle size of 108.9 nm, entrapment efficiency of 78.62% and *in vitro* drug release of 98.88% at 36 h in pH 7.4 PBS. The optimized formulation possessed an optimum PDI of 1.217 and a stable ZP of -24.3 mV with roughly spherical shape. Further, its targeting to brain after oral administration was confirmed by fluorescence microscopy studies. The prepared COF were showed that non-toxic up to 125µg/ml by MTT Assay. Hence, surface modified SLNs are potential novel drug delivery system for Asenapine Maleate to increase its bioavailability and brain targeting.

DISCLAIMER

The products used for this research are commonly and predominantly use products in our research area and country. There is absolutely no conflict of interest between the authors and producers of the products because we do not intend to use these products as an avenue for any litigation but for the advancement of knowledge. Also, the research was not funded by the producing company rather it was funded by personal efforts of the authors.

FUTURE PROSPECTIVE

The concentration of tween 80 for surface modifications has to be assessed.

CONSENT

It is not applicable.

ETHICAL APPROVAL

All authors hereby declare that all experiments have been examined and approved by the appropriate ethics committee and have therefore been performed in accordance with the ethical standards laid down in the 1964 Declaration of Helsinki.

ACKNOWLEDGEMENT

The authors are indebted to Sri Padmavathi School of Pharmacy, Tiruchanoor for supporting completion of this research work. I would like to acknowledge DST-FIST, Institute of Pharmaceutical Technology, Sri Padmavathi Mahila Visvavidyalayam, Tirupati. Sophisticated Analytical Instruments Facility (SAIF), Panjab University, Chandigarh. SAIF, IITM, Chennai. Sri Vidynikethan College of Pharmacy, A.Rangampeta for supporting the samples analysis.

COMPETING INTERESTS

Authors have declared that no competing interests exist.

REFERENCES

1. Talegaonkar S, Bhattacharyya A. Potential of Lipid Nanoparticles (SLNs and NLCs) in Enhancing Oral Bioavailability of Drugs with Poor Intestinal Permeability, AAPS Pharm Sci Tech. 2019;20(3):121. DOI: 10.1208/s12249-019-1337-8.
2. Manish G, Verma M, Chauhan I, Yasir M, Pratap Singh A, Pawan Kumar S, Solid Lipid Nanoparticles for Oral Drug Delivery: A Review, Curr Nano. 2020;10(3):208-224. DOI: 10.2174/2468187310666200221105315.
3. Blasi P, Giovagnoli S, Schoubben A, Ricci M, Rossi C, Solid lipid nanoparticles for targeted brain drug delivery. Adv Drug Del Rev. 2007;59:454–477. DOI: 10.1016/j.addr.2007.04.011.
4. Santosh AK, Chandrakant RK, Birendra S, Bapi G, Hira C, Preparation, characterization, and optimization of asenapine maleate mucoadhesive nanoemulsion using Box-Behnken design: *In vitro* and *in vivo* studies for brain targeting. Int. J Pharmaceutics. 2020;586:1-15.119499. DOI: 10.1016/j.ijpharm.2020.119499.
5. Available:https://www.accessdata.fda.gov/drugsatfda_docs/label/2011/022117s010lbl.pdf.
6. Managuli RS, Wen Wang JT, Faruq FM, Abhjieet P, Jain S, Al-Jamal KT, Srinivas M, Surface engineered nanoliposomal

platform for selective lymphatic uptake of asenapine maleate: *In vitro* and *in vivo* studies. Materials Sci & Eng C. 2020;109:1-13.Article No-110620. DOI.org/10.1016/j.msec.2019.110620

7. Dhudipala N, Karthikyadav J. Lipid nanoparticles of zaleplon for improved oral delivery by Box-Behnken design: Optimization, *in vitro* and *in vivo* evaluation. Drug Dev and Ind Pharm. 2017; 1-27. DOI.org/10.1080/03639045.2017.1304957
8. Suryateja SP, Mothilal M, Damodharan N, Jaison D. Screening and Optimization of Valacyclovir Niosomes by Design of Experiments. Int. J Appl Pharmaceutics. 2018;10(1):79-85. DOI.org/10.22159/ijap.2018v10i1.22566.
9. Rahman Z, Ahmed SZ, Khan MA. Non-destructive methods of characterization of risperidone solid lipid nanoparticles. Eur J Pharma and Biopharm. 2010;76(2010):127–137. DOI: 10.1016/j.ejpb.2010.05.003.
10. Gidwani B, Vyas A. Preparation, characterization, and optimization of Altretamine-loaded solid lipid nanoparticles using Box-Behnken design and response surface methodology. Artificial Cells, Nanomed and Biotech. 2014;44(2):571-580. DOI.org/10.3109/21691401.2014.971462.
11. Vijayavani SCh, Vidyavathi M. Azadirachita indica gum based sildenafil citrate mucoadhesive microspheres – Design and optimization. J Drug Deli Sci and Tech. 2018;47(2018):499-513. DOI: 10.1016/j.jddst.2018.08.011
12. Smriti O, Babita K. Preparation and Statistical Modelling of Solid Lipid Nanoparticles of Dimethyl Fumarate for Better Management of Multiple Sclerosis. Adv Pharm Bull. 2018;8(2):225-233. DOI.org/10.15171%2Fapb.2018.027
13. Safal J, Sanjay J, Piush K, Arvind G, Divya B, Jain SK. Design and development of solid lipid nanoparticles for topical delivery of an anti-fungal agent. Drug Deliv. 2010;17(6):443–451. DOI: 10.3109/10717544.2010.483252.
14. Gupta S, Rajesh K, Narendra C, Misra A, Abdelwahab O. Systematic Approach for the Formulation and Optimization of Solid Lipid Nanoparticles of Efavirenz by High Pressure Homogenization Using Design of Experiments for Brain Targeting and Enhanced Bioavailability. Hindawi BioMed Res Int, 2017;2017:1-18. Article ID 5984014. DOI.org/10.1155/2017/5984014
15. Gulbake A, Jain A, Piush K, Jain SK. Solid lipid nanoparticles bearing oxybenzone: In-vitro and in-vivo evaluation. J Microencaps. 2010;27(3):226–233. DOI.org/10.3109/02652040903067844.
16. Devi R, Jain A, Hurkat P, Jain SK. Dual Drug Delivery Using Lactic Acid Conjugated SLNs for Effective Management of Neurocysticercosis. Phar Res. 2015;32:10. DOI: 10.1007/s11095-015-1677-3.
17. Yadav P, Goutam R, Gazal S, Ranjit S and Amit Kumar G. Polysorbate 80 Coated Solid Lipid Nanoparticles for the Delivery of Temozolomide into the Brain. The Open Pharmacol J. 2018; 8:21-2. Available:http://dx.doi.org/10.2174/1874143601808010021
18. Saupe A, Gordon KC, Thomas R. Structural investigations on nanoemulsions, solid lipid nanoparticles and nanostructured lipid carriers by cryo-field emission scanning electron microscopy and Raman spectroscopy. Intl J Pharma. 2006;314(2006):56–62. Available: https://aif.csio.res.in/fesem. DOI: 10.1016/j.ijpharm.2006.01.022.
19. Shrotriya SN, Bhagvat VV, Manasi SS. Formulation and development of Silybin loaded solid lipid nanoparticle enriched gel for irritant contact dermatitis. J of Drug Deliv Sci and Tech. 2017; 41:164-173. Available:https://doi.org/10.1016/j.jddst.2017.07.006
20. Behbahani ES, Ghaedi M, Abbaspour M, Rostamizadeh K. Optimization and characterization of ultrasound assisted preparation of curcumin-loaded solid lipid nanoparticles: Application of central composite design, thermal analysis and X-ray diffraction techniques. Ultrason Sonochem. 2017;38:271-280. DOI: 10.1016/j.ultsonch.2017.03.013.
21. Kharya P, Ashish J, Arvind G, Satish S, Ankit J, Pooja H, Subrata M, Jain SK. Phenylalanine-coupled solid lipid nanoparticles for brain tumor targeting. J Nano Res. 2013;15:2022:1-12. DOI 10.1007/s11051-013-2022-6.
22. Kuo YC, Su-FL. Transport of stavudine, delavirdine, and saquinavir across the blood–brain barrier by polybutyl cyano

acrylate, methyl methacrylate-sulfo propyl methacrylate, and solid lipid nanoparticles. Int J of Pharm. 2007;340(2007):143–152. DOI: 10.1016/j.ijpharm.2007.03.012.

23. Shi, Li-Li, Cao, Yue, Zhu, Xiao-Yin, Cui, Jing-Hao, Cao, QingRi, Optimization of process variables of zanamivir-loaded solid lipid nanoparticles and the prediction of their cellular transport in Caco-2 cell model, Int J of Pharm. 2015;478(1):60-69. Available:http://dx.doi.org/10.1016/j.ijpharm.2014.11.017
24. Suryateja SP, N. Damodharan. 2^3 Full Factorial Model for Particle Size Optimization of Methotrexate Loaded Chitosan Nanocarriers: A Design of Experiments (DoE) Approach. Hindawi. BioMed Res Int. 2018;1-9. Available:https://doi.org/10.1155/2018/7834159
25. Kim BD, Hoo-Kyun C. Preparation and characterization of solid lipid nanoparticles (SLN) made of cacao butter and curdlan. Eur J Pharm Sci. 2005;24(2-3):199-205. DOI: 10.1016/j.ejps.2004.10.008.
26. Helgason T, Awad TS, Bergsson KK, Clements DJM, Weiss J. Effect of surfactant surface coverage on formation of solid lipid nanoparticles (SLN). J Colloid Interface Sci. 2009; 334(1):75-81. DOI: 10.1016/j.jcis.2009.03.012
27. Behbahani ES, Ghaedi M, Abbaspour M, Rostamizadeh K. Optimization and characterization of ultrasound assisted preparation of curcumin-loaded solid lipid nanoparticles: Application of central composite design, thermal analysis and X-ray diffraction techniques. Ultrason Sonochem. 2017;38:271-280. DOI:10.1016/j.ultsonch.2017.03.013.
28. Yasir M, Sara UVS. Preparation and optimization of haloperidol loaded solid lipid nanoparticles by Box-Behnken design. J Pharm Res. 2013;7(5):551-558. Available:https://dx.doi.org/10.1016%2Fj.apsb.2014.10.005.
29. Ang BC, Yaacob II, Irwan N. Investigation of Fe_2O_3/SiO_2 Nanocomposite by FESEM and TEM. Hindawi. J Nano. 2013;1-6. Article ID 980390. DOI.org/10.1155/2013/980390.
30. Almeida JP, Chen AL, Foster A, Drezek R. *In vivo* biodistribution of nanoparticles, Nanomedicine (Lond). 2011;6(5):815-35. DOI: 10.2217/nnm.11.79.
31. Bailly AL, Correard F, Popov A, Selikov GT, Chaspoul F, Appay R, Kattan A, Kabashin AV, Braguer D, Esteve MA. *In vivo* evaluation of safety, biodistribution and pharmacokinetics of laser synthesized gold nanoparticles. Scientific Reports, Natur Sear. 2019;9(12890)1-12. DOI.ORG/10.1038/S41598-019-48748-3.
32. Patel M, Veenu M, Sawant K. Enhanced intestinal absorption of asenapine maleate by fabricating solid lipid nanoparticles using TPGS: elucidation of transport mechanism, permeability across Caco-2 cell line and in-vivo pharmacokinetic studies, Artificial Cells, Nanomed and Biotech. 2019;47(1):144-153. DOI: 10.1080/21691401.2018.1546186.

Peer-review history:
The peer review history for this paper can be accessed here:
http://www.sdiarticle4.com/review-history/69419